Analysis Of Optimum Corner Radius Of Electrolyte Flow Path In Ecm Using CFD

Krishna Mohan Singh[1], R. N. Mall[2]

1. M.Tech. Final Year CIM, MMMEC Gorakhpur

2. Asstt. Professor, MMMEC Gorakhpur

Abstract-The main objective of the paper is to investigate the flow pattern of electrolyte in the flow path for sharp corners and rounded corners (radius from 0.6-0.9mm) and to suggest the best geometry for flow path with the help of CFD. Pressure distribution (contours), velocity vectors,path lines etc. have been obtained for the flow path of electrolyte.

1.0INTRODUCTION

Electrochemical Machining (ECM) is an un-conventional machining (UCM) process which belongs to electrochemical category. UCM is opposite of galvanic or electrochemical coating or deposition process. Hence UCM can be thought of a controlled anodic dissolution at atomic level of the work piece that is electrically conductive by a shaped tool owing to flow of high current at relatively low potential difference through an electrolyte.
New concept of manufacturing uses non-traditional energy sources like light, sound, mechanical, electrical, chemical, ions and electrons. With the technological and industrial growth, development of difficult to machine and harder materials, finding applications in nuclear engineering, aerospace and other industries having high strength to weight ratio, heat resistance, hardness etc qualities. The new developments in the field of material science leading to new engineering metallic materials, high tech ceramics and composite materials having good mechanical properties and thermal characteristics apart from having sufficient electrical conductivity so that they can be easily machined by spark erosion. UCM has grown out of the need to machine these types of exotic materials. Non-traditional machining processes are non-traditional in the sense that they do not use traditional tools for machining and instead these machining processes directly use other forms of energy. High complexity in shape, higher demand for product accuracy, size, and surface finish etc problems can be solved using non-traditional or un-conventional methods. The un-conventional machining processes possess virtually unlimited capabilities except for volumetric material removal rates, for which great advances have been made in the past few years to enhance the material removal rates. Since material removal rate increases, cost effectiveness of operations also increases that stimulate greater uses of un-conventional machining processes.

1.1 FUNDAMENTAL PRINCIPLES OF ECM

During Electro chemical machining, there are reactions occurring at the electrodes i.e. at the anode that is work-piece and at the cathode that is tool along with within electrolyte. Electrons and Ion crossing phase boundaries (the interface between two or more separate phases, such as liquid-solid) would result in electron transfer reaction carried out at both anode and cathode.

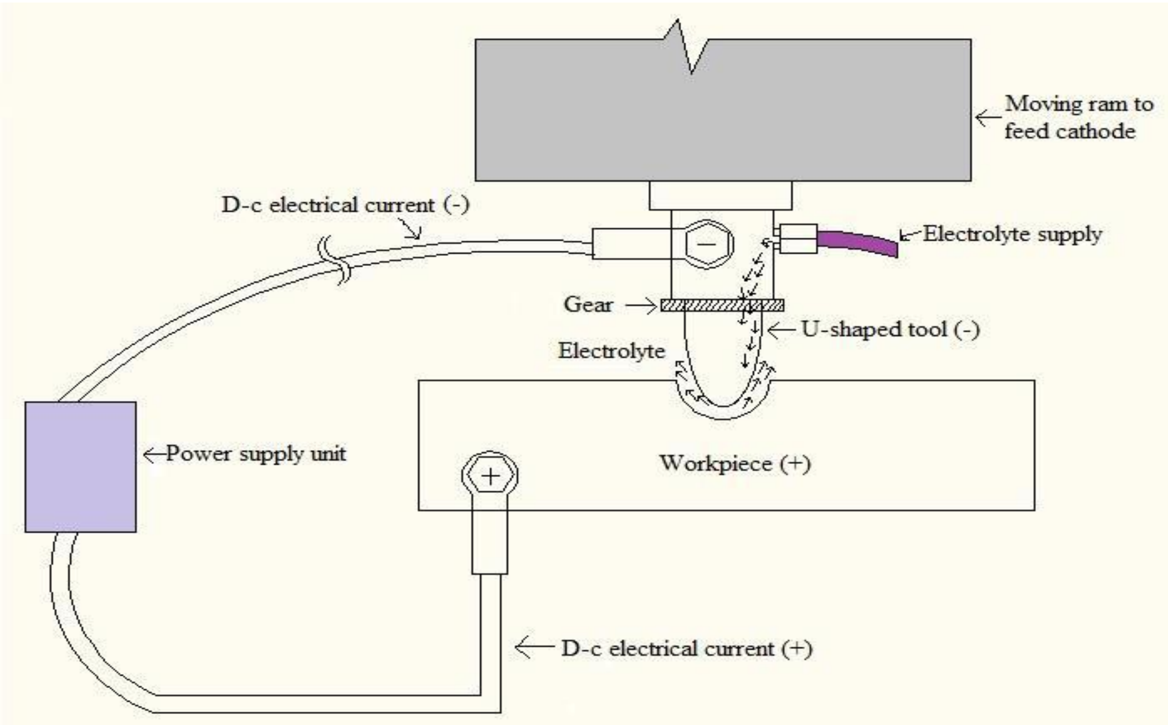

Figure 1.1: Principle of Electrochemical Machining

In the mean time, the potential difference is fundamental in understanding the energy distribution during the ECM process. Fig. 1.2 shows the wide concepts and basic potential calculation methods. Nernst equation is used to calculate the electrode reversible potential. Tafel equation, diffusion layer, and ohm's law can assist in estimating activation over potential, concentration over potential, and resistance over potential, which are known as the three main over potentials in electrochemical reactions.

1.2 CHARACTERSTICS OF ELECTROCHEMICAL MACHINING PROCESS

Material removal mechanism controlled removal of metal by anodic dissolution in an electrolytic medium. It consists of advantage of ECM, Disadvantage of ECM and application of ECM.

Table-1.1 ECM specification

Tool	Copper, brass or steel
Power supply	Constant voltage 5-30 DC volt
Current	50-40,000 amp
Material removal rate	1600 mm3/min
Specific power consumption	7w/mm3/min
Electrolytic solution	Neutral salt, brine solution,
Accuracy and surface finish	0.02 mm, 0.4µm
Application	Machining hard material
Limitation	High specific energy consumption
Mechanical properties	Stress free machining, reduce tool wear
Surface properties	No thermal damage

1.3 Advantage of ECM

Electrochemical machining is a promising alternative if conventional mechanical manufacturing processes reach technical as well as economical limitations. Nowadays, ECM is established for burr removing, shape manufacturing and drilling of jet engine parts. Considering these advantages ECM is a suitable technique for machining mechanical hard to cut materials such as carbide metals or cermets.

[1] No mechanical stress impact into the processed work piece.
[2] No thermal impact of the work piece.
[3] The removal rate is not determined by the hardness and toughness of the material.
[4] No process related tool wear.
[5] Great versatility for machining of geometrical complex shapes.
[6] No burr formation.

1.4 Disadvantages of ECM

[1] High specific energy consumption.
[2] Not suited for non-conducting pieces.
[3] High initial and working cost.

1.5 Application of ECM

ECM technique removes material by atomic level dissolution of the same by electrochemical action. Thus the material removal rate or machining is not dependent on the mechanical or physical properties of the work material. It only depends on the atomic weight and valency of the work material and the condition that it should be electrically conductive. Thus ECM can machine any electrically conductive work material irrespective of their hardness, strength or even thermal

properties. Moreover as ECM leads to atomic level dissolution, the surface finish is excellent with almost stress free machined surface and without any thermal damage.
ECM is used for:

- Die sinking (Fig 1.4)
- Profiling and contouring (Fig 1.5)
- Trepanning (Fig 1.7)
- Grinding
- Drilling (Fig 1.6)
- Micro-machining

2.0 Modeling of Flow Domain

2.1 Geometric Modeling of Flow Domain

The geometry and flow domain of the electrolyte flow path is modeled by using GAMBIT 2.3.16 software. The geometry modeling and meshing tool of GAMBIT allows us for creation and manipulation of highly complex geometries and mesh generation.

2.2 Selection of Solver

Pressure based or segregated solver is selected for solving incompressible flow through the electrolyte path with implicit scheme with cell based approach. 2D approach is used.

2.3 Boundary Conditions

For solving any problem using numerical technique, it is first step to apply appropriate and exact boundary conditions, which defines the problem, in order to get the solution of that specific problem. A solution is always sensitive to the inlet boundary conditions; a great care is needed to be taken while imposing the boundary condition.

After meshing the domain, it is imported to the solver “FLUENT” version 6.3.26.The dimensions of the domain properly scaled (conversion from cm to meter). The pressure based or segregated solver is used for the current problem.

Primarily the standard k-ε model is used for viscous modeling, after a converged result it is switched over to other model to find out the appropriate viscous model suitable for the present case.

2.4 Boundary Conditions: VELOCITY_INLET- is given at the inlet of the tool

Pressure outlet – is given at the outlet of the electrolyte flow

WALL – is selected for all other sections

FLUID- is specified as continuum type boundary condition.

2.5 Properties of Electrolyte used:

Density of electrolyte (ρ) = 1050 kg/m^3

Dynamic viscosity of water (μ) = 0.001 kg/m-sec.

2.6 Calculations:

Electrolyte flow in the ECM flow path can be recognized by calculating Reynold's number, which is given as (using equation equation 4.1)

$$R_N = \frac{VD\rho}{\mu} \qquad \text{...(4.1)}$$

R_N = Reynolds's number

V = Mean Velocity of flow

D = diameter of tubular flow

μ = Kinematics Viscosity (Dynamic viscosity / Density)

ρ = Fluid density

When the Reynolds No. (R_N) is less than 2000 fluid flow results in laminar flow and if the Reynolds No. (R_N) is more than 2000 turbulent flow occurs.

Table 4.1: Different values of inlet velocity

S.N.	Inlet Velocity (m/s)
1.	5
2.	15
3.	30
4.	50

Calculation-1

For Electrolyte

Density of fluid (ρ) = 1050 kg/m^3

Dynamic viscosity of water (μ) = 0.001 kg/m-sec.

Inlet diameter of electrolyte=2mm=0.002m

Inlet velocity=5 m/s

Substituting above values in equation 1.1

$R_N = \frac{1050 X .002 X 5}{0.001}$=10500 (turbulent flow)

Calculation-2

For Inlet velocity=15 m/s

Substituting above values in equation 1.1

$R_N = \frac{1050 X 0.002 X 15}{0.001}$=31500 (turbulent flow)

Calculation-3

For Inlet velocity=30 m/s

Substituting above values in equation 1.1

$R_N = \frac{1050 X 0.002 X 30}{0.001}$=63000 (highly turbulent flow)

Calculation-4

For Inlet velocity=50m/s

Substituting above values in equation 1.1

$R_N = \frac{1050 X 0.002 X 50}{0.001}$=105000 (highly turbulent flow)

RESULTS AND DISCUSSION FROM CFD ANALYSIS

For sharp corners and rounded corners, flow has been simulated for inlet velocity of 5m/s, 15m/s, 30m/s and 50m/s. For the entire inlet velocities corresponding Reynolds no. are 10500, 31500, 63000 and 105000, which shows the turbulent flow for all inlet velocity range.

For rounded corners 0.6mm, 0.7mm, 0.8mm and 0.9mm radius have been used.

For above inlet velocity range $k-\varepsilon$ model are more appropriate rather than other models available in FLUENT.

Hence for simulation of electrolyte flow, standard $k-\varepsilon$ model with standard wall functions and standard $k-\varepsilon$ model with enhanced wall treatment has been used for all cases.

The gap between tool and work piece is maintained at 0.8mm

Discussion on results for flow through sharp corners

Electrolyte flow through sharp corners has been simulated for the inlet velocity of 5m/s, 15m/s, 30m/s and 50m/s.

By using standard $k-\varepsilon$ model with standard wall functions and standard $k-\varepsilon$ model with enhanced wall treatment separately for above mentioned velocity range pressure contours, velocity contours, velocity vectors and path lines has been obtained.

With the help of above figures results have been tabulated in Table 5.1

Table 5.1 shows possibility of vortex formation and negative pressure for sharp corners flow path.

We can observe from Table 5.1 and from fig.4.6 to fig.4.37 that for entire velocity range (5 to 50m/s) and for both standard $k-\varepsilon$ model with standard wall functions and standard $k-\varepsilon$ model with enhanced wall treatment, sharp corners produces negative pressure and vortex inside flow path.

These vortex formation and stagnation of flow affects the surface of work.

Discussion on results for flow through rounded corner of radius 0.6mm

Electrolyte flow through rounded corner of radius 0.6mm has been simulated for the inlet velocity of 5m/s, 15m/s, 30m/s and 50m/s.

By using standard $k-\varepsilon$ model with standard wall functions and standard $k-\varepsilon$ model with enhanced wall treatment separately for above mentioned velocity range pressure contours, velocity contours, velocity vectors and path lines has been obtained.

With the help of above figures results have been tabulated in Table 5.2

From Table 5.2 we can observe that at low inlet velocity i.e. 5m/s, there is no negative pressure and vortex formation inside flow path.

For 15m/s inlet velocity there is negligible negative pressure and vortex formation inside flow path.

If we further proceed to higher inlet velocities i.e. 30m/s and 50m/s there is negative pressure present inside flow path but the vortex formation is negligible i.e. invisible.

We can also observe from table 5.2 that both the model combination (standard $k-\varepsilon$ model with standard wall functions and standard $k-\varepsilon$ model with enhanced wall treatment) produces almost same results for entire velocity range.

Discussion on results for flow through rounded corner of radius 0.7mm

Electrolyte flow through rounded corner of radius 0.7mm has been simulated for the inlet velocity of 5m/s, 15m/s, 30m/s and 50m/s.

By using standard $k-\varepsilon$ model with standard wall functions and standard $k-\varepsilon$ model with enhanced wall treatment separately for above mentioned velocity range pressure contours, velocity contours, velocity vectors and path lines has been obtained.

With the help of above figures results have been tabulated in Table 5.3

From Table 5.3 we can observe that at low inlet velocity i.e. 5m/s, there is no negative pressure and vortex formation inside flow path.

If we further proceed to higher inlet velocities i.e. 15m/s, 30m/s and 50m/s there is negative pressure present inside flow path but the vortex formation is negligible i.e. invisible in figures.

We can also observe from table 5.3 that both the model combination (standard $k-\varepsilon$ model with standard wall functions and standard $k-\varepsilon$ model with enhanced wall treatment) produces almost same results for entire velocity range.

Discussion on results for flow through rounded corner of radius 0.8mm

Electrolyte flow through rounded corner of radius 0.8mm has been simulated for the inlet velocity of 5m/s, 15m/s, 30m/s and 50m/s.

By using standard $k-\varepsilon$ model with standard wall functions and standard $k-\varepsilon$ model with enhanced wall treatment separately for above mentioned velocity range pressure contours, velocity contours, velocity vectors and path lines has been obtained.

With the help of above figures results have been tabulated in Table 5.4

From Table 5.4 we can observe that at inlet velocity of 5m/s and 15m/s, there is no negative pressure and vortex formation inside flow path.

If we further proceed to higher inlet velocities i.e. 30m/s and 50m/s there is negative pressure present inside flow path but the vortex formation is negligible i.e. invisible in figures.

We can also observe from table 5.4 that both the model combination (standard $k-\varepsilon$ model with standard wall functions and standard $k-\varepsilon$ model with enhanced wall treatment) produces almost same results for entire velocity range.

Discussion on results for flow through rounded corner of radius 0.9mm

Electrolyte flow through rounded corner of radius 0.9mm has been simulated for the inlet velocity of 5m/s, 15m/s, 30m/s and 50m/s.

By using standard $k-\varepsilon$ model with standard wall functions and standard $k-\varepsilon$ model with enhanced wall treatment separately for above mentioned velocity range pressure contours, velocity contours, velocity vectors and path lines has been obtained.

With the help of above figures results have been tabulated in Table 5.5

From Table 5.5 we can observe that at inlet velocity of 5m/s there is no negative pressure and vortex formation inside flow path.

For inlet velocity of 15m/s standard $k-\varepsilon$ model with standard wall functions shows that there is negative pressure present inside flow path but the vortex formation is negligible i.e. invisible but standard $k-\varepsilon$ model with enhanced wall treatment shows that there is no negative pressure and vortex formation inside flow path.

If we further proceed to higher inlet velocities i.e. 30m/s and 50m/s there is negative pressure present inside flow path but the vortex formation is negligible i.e. invisible in figures.

LIST OF FIGURES

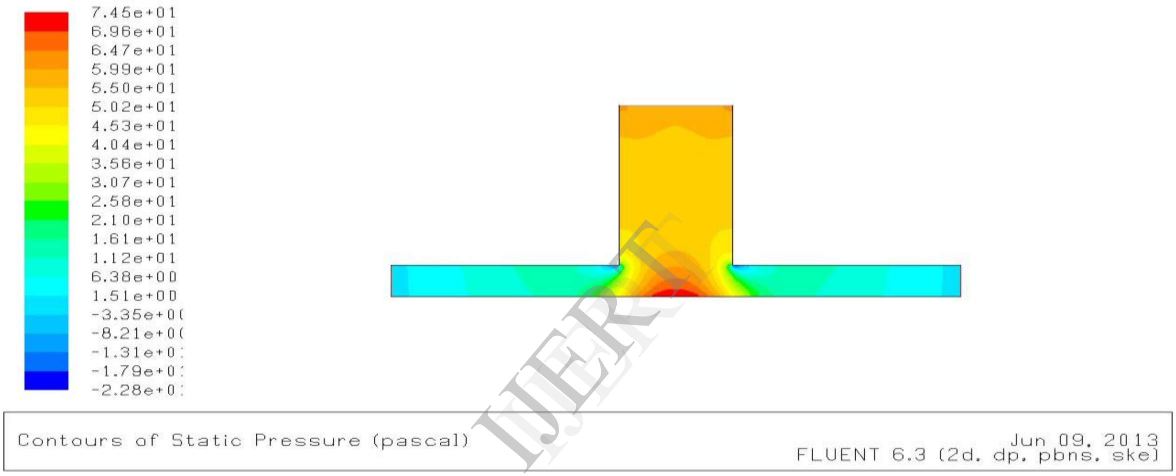

Figure 5.1: Contours of static pressure for electrolyte flow path with sharp corners at inlet velocity, V=5m/s [$k-\varepsilon$ model with standard wall functions]

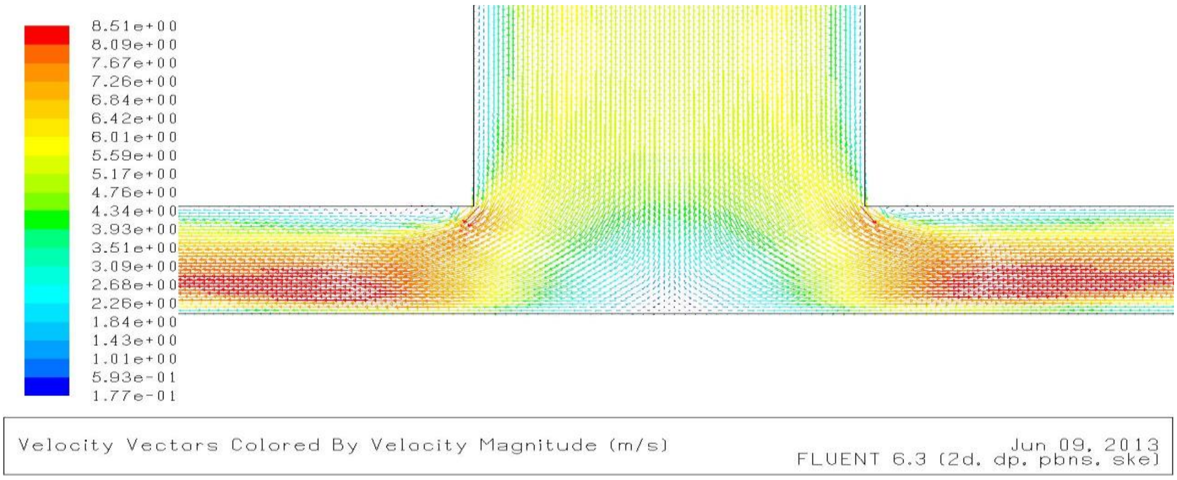

Figure 5.2: velocity vectors for electrolyte flow path with sharp corners at inlet velocity, V=5m/s [$k-\varepsilon$ model with standard wall functions]

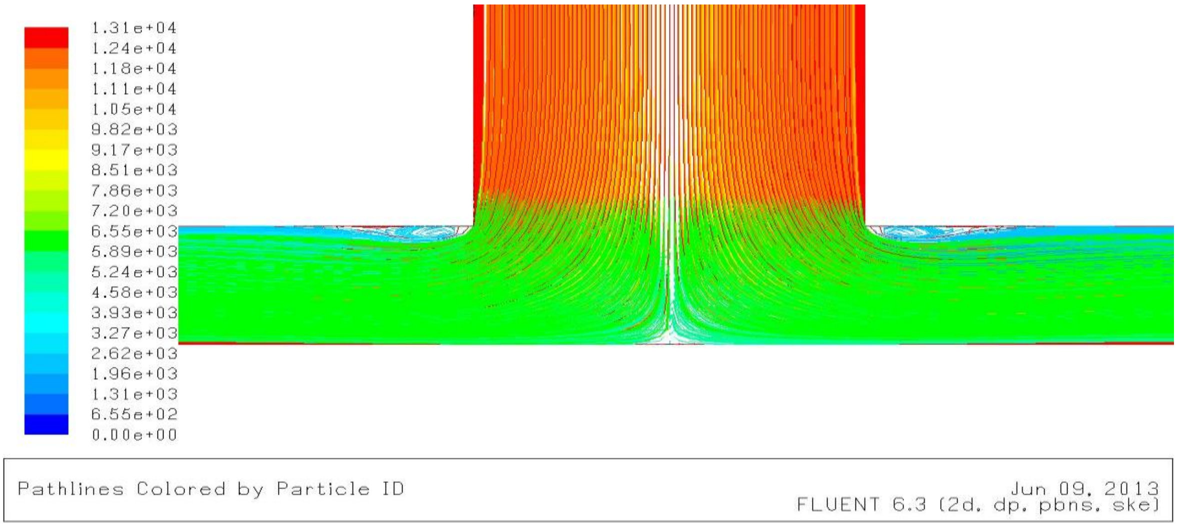

Figure 5.3: path lines for electrolyte flow path with sharp corners at inlet velocity, V=5m/s [$k-\varepsilon$ model with standard wall functions]

Figure 5.4: Contours of static pressure for electrolyte flow path with corner radius of 0.6mm at inlet velocity, V=5m/s [$k-\varepsilon$ model with standard wall functions]

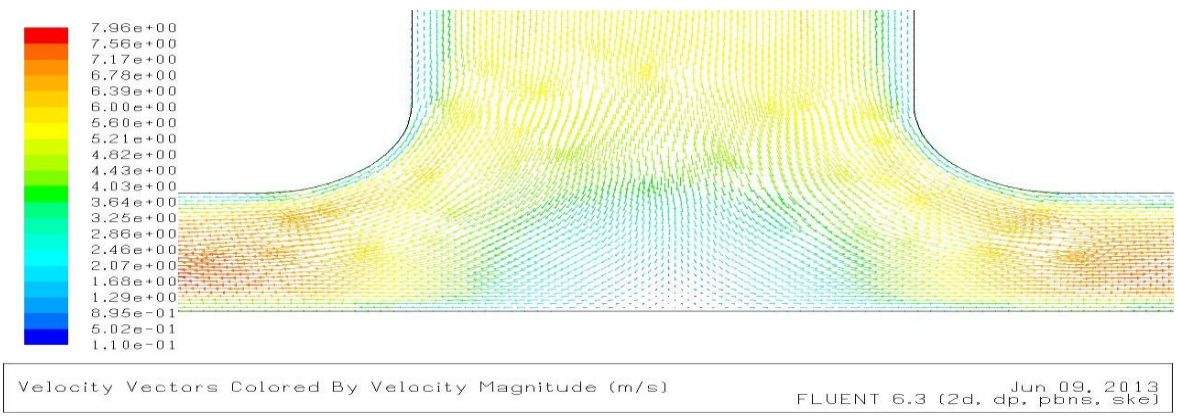

Figure 5.5: velocity vectors for electrolyte flow path with corner radius of 0.6mm at inlet velocity, V=5m/s [$k-\varepsilon$ model with standard wall functions]

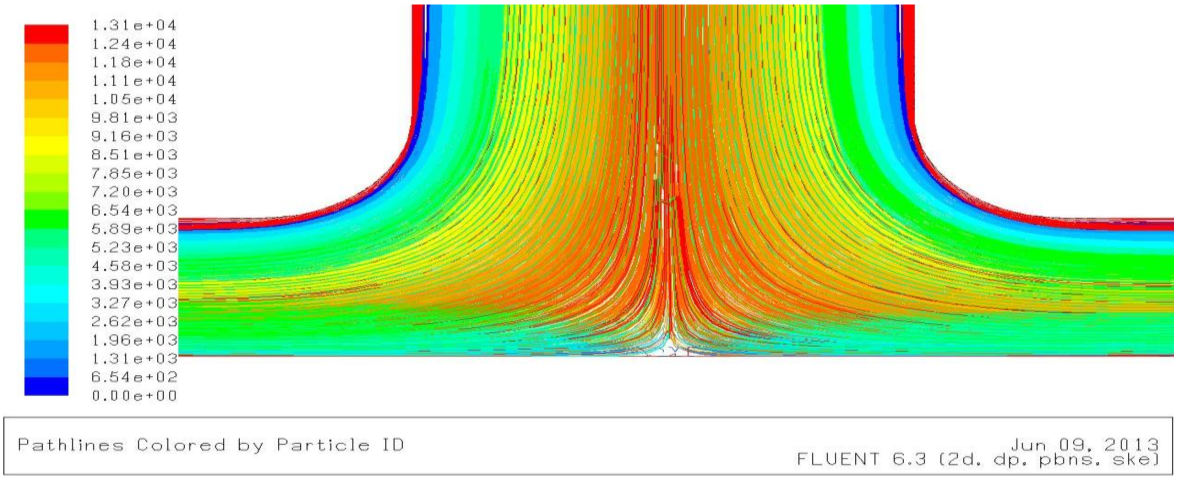

Figure 5.6: path lines for electrolyte flow path with corner radius of 0.6mm at inlet velocity, V=5m/s [$k-\varepsilon$ model with standard wall functions]

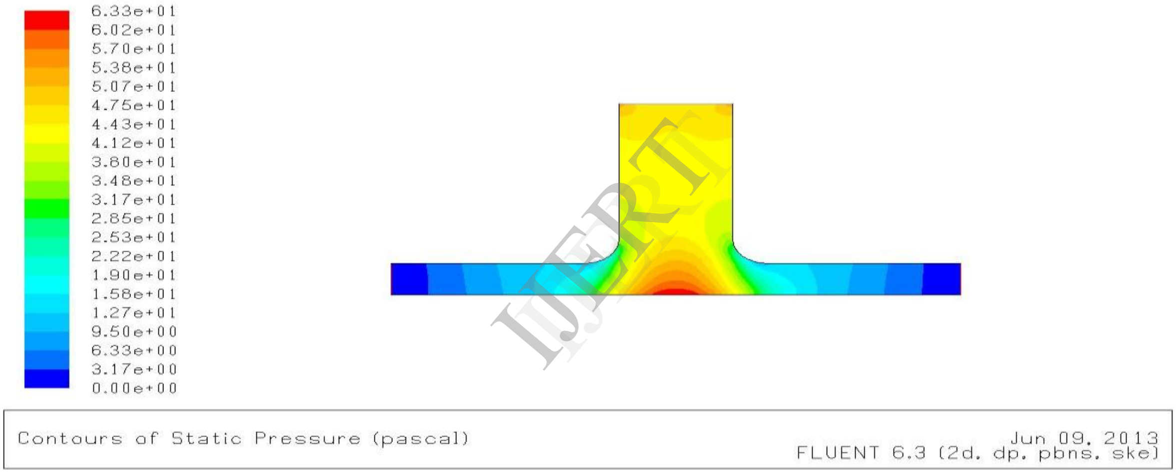

Figure 5.7: Contours of static pressure for electrolyte flow path with corner radius of 0.7mm at inlet velocity, V=5m/s [$k-\varepsilon$ model with standard wall functions]

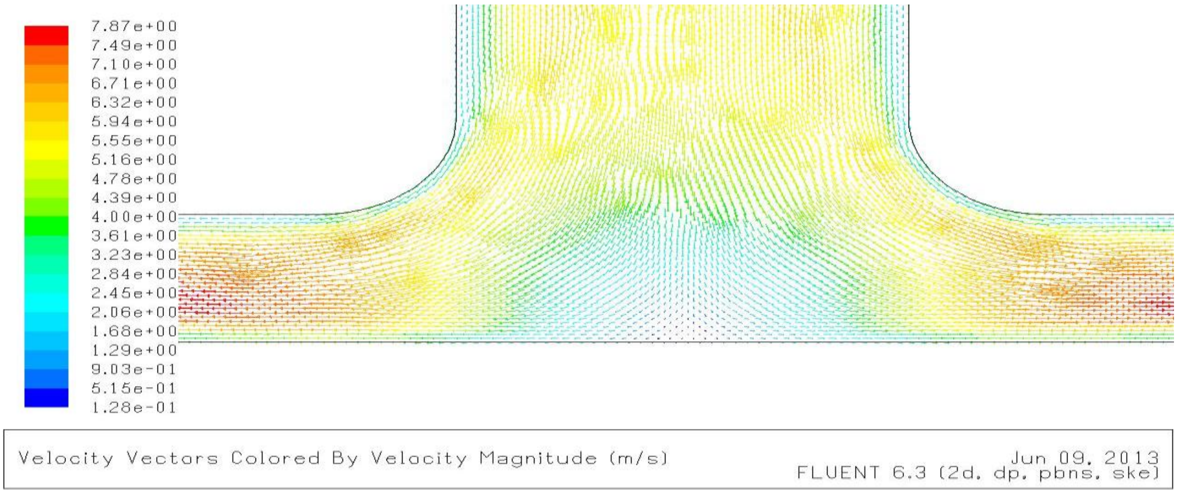

Figure 5.8: velocity vectors for electrolyte flow path with corner radius of 0.7mm at inlet velocity, V=5m/s [$k-\varepsilon$ model with standard wall functions]

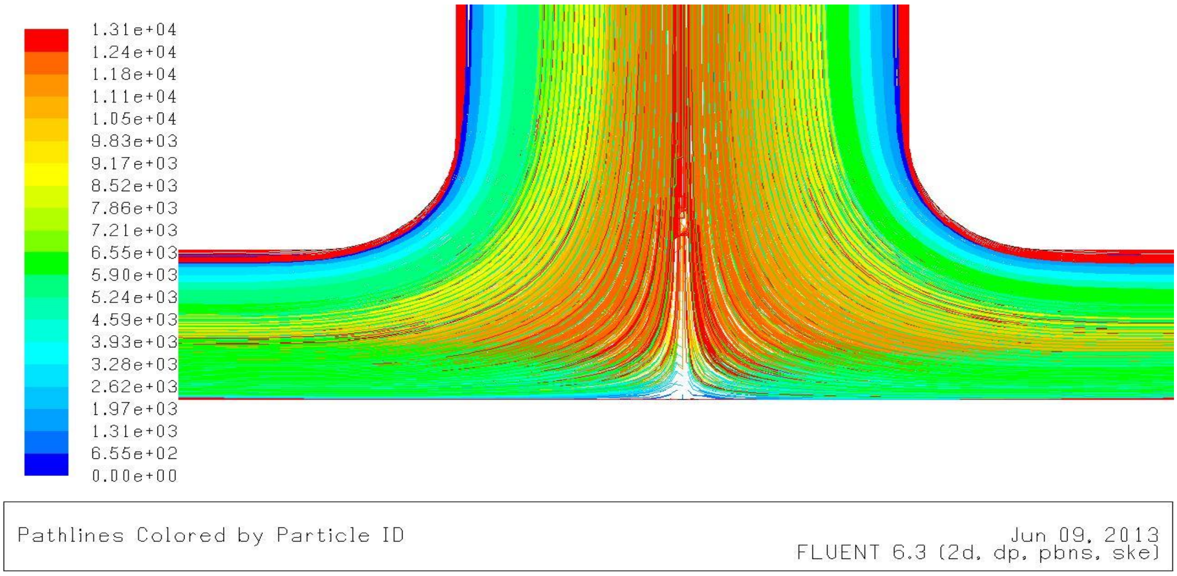

Figure 5.9: path lines for electrolyte flow path with corner radius of 0.7mm at inlet velocity, V=5m/s [$k-\varepsilon$ model with standard wall functions]

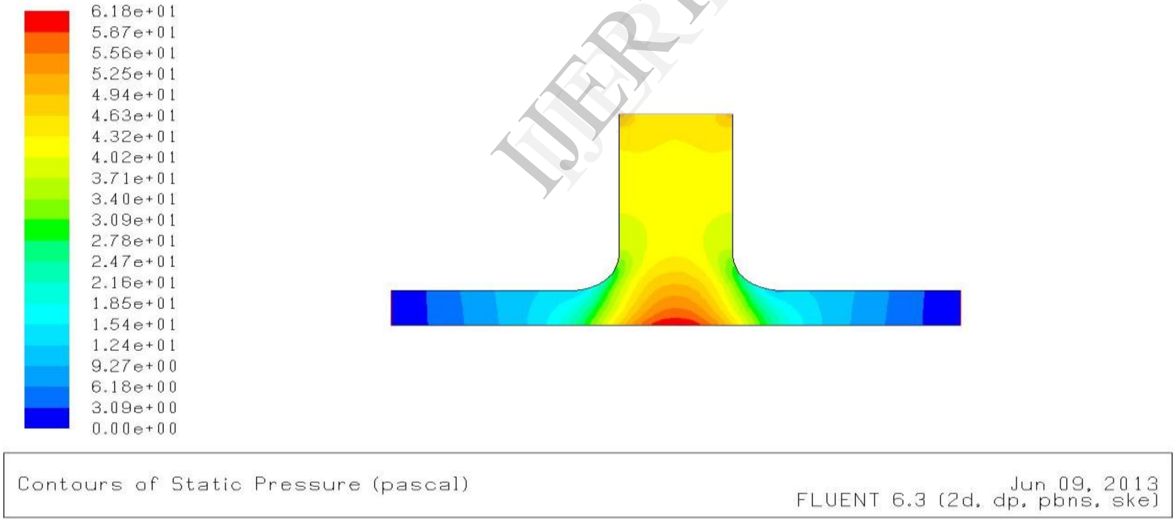

Figure 5.10: Contours of static pressure for electrolyte flow path with corner radius of 0.8mm at inlet velocity, V=5m/s [$k-\varepsilon$ model with standard wall functions]

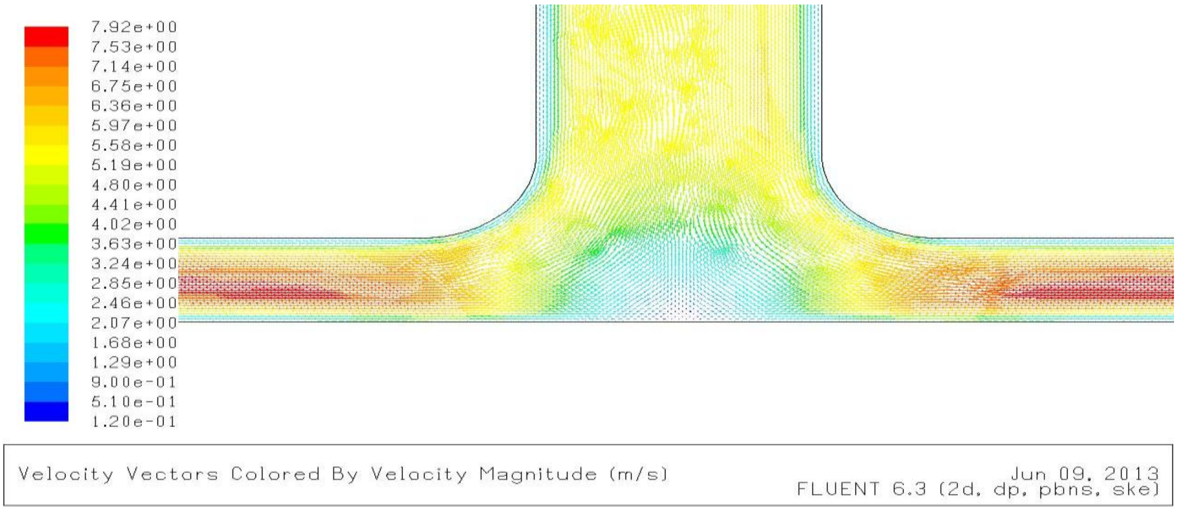

Figure 5.11: velocity vectors for electrolyte flow path with corner radius of 0.8mm at inlet velocity, V=5m/s [$k - \varepsilon$ model with standard wall functions]

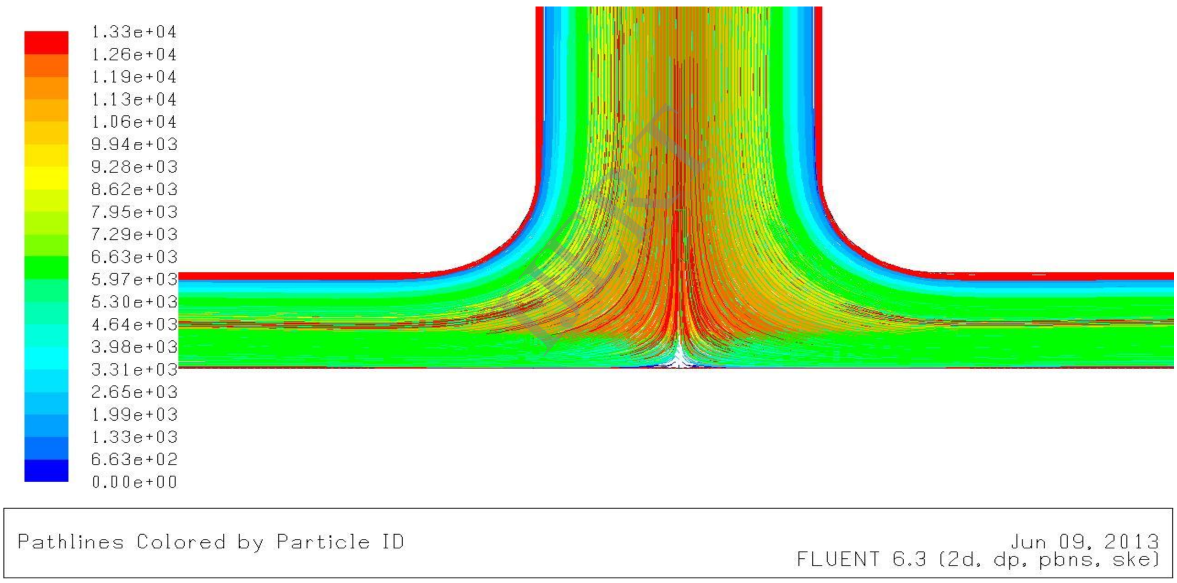

Figure 5.12: path lines for electrolyte flow path with corner radius of 0.8mm at inlet velocity, V=5m/s [$k - \varepsilon$ model with standard wall functions]

ISSN: 2278-0181
Vol. 2 Issue 7, July - 2013

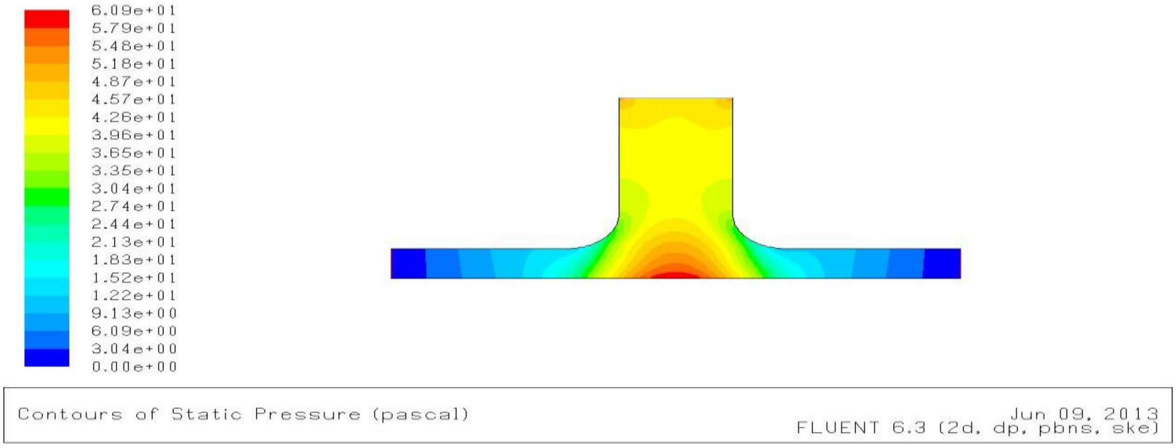

Figure 5.13: Contours of static pressure for electrolyte flow path with corner radius of 0.9mm at inlet velocity, V=5m/s [$k-\varepsilon$ model with standard wall functions]

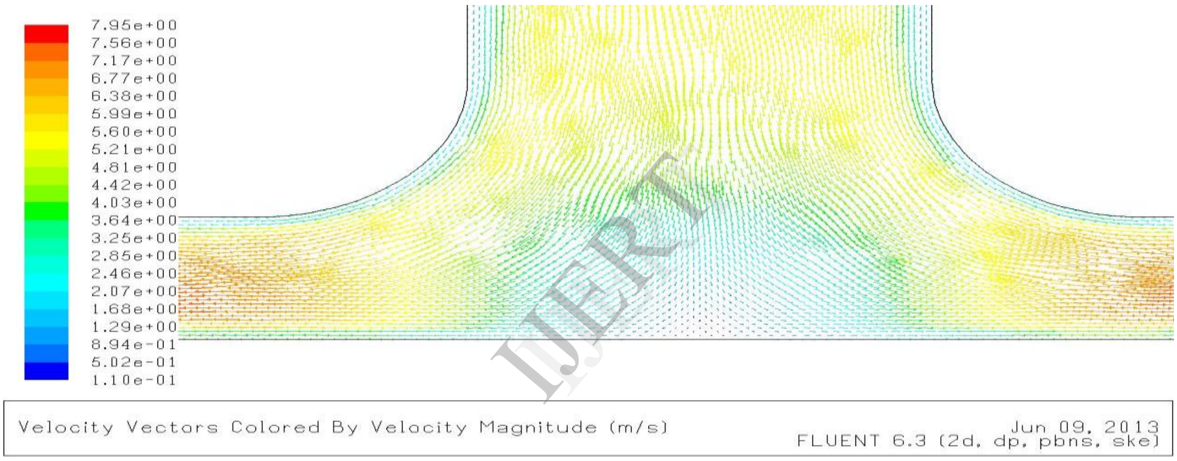

Figure 5.14: velocity vectors for electrolyte flow path with corner radius of 0.9mm at inlet velocity, V=5m/s [$k-\varepsilon$ model with standard wall functions]

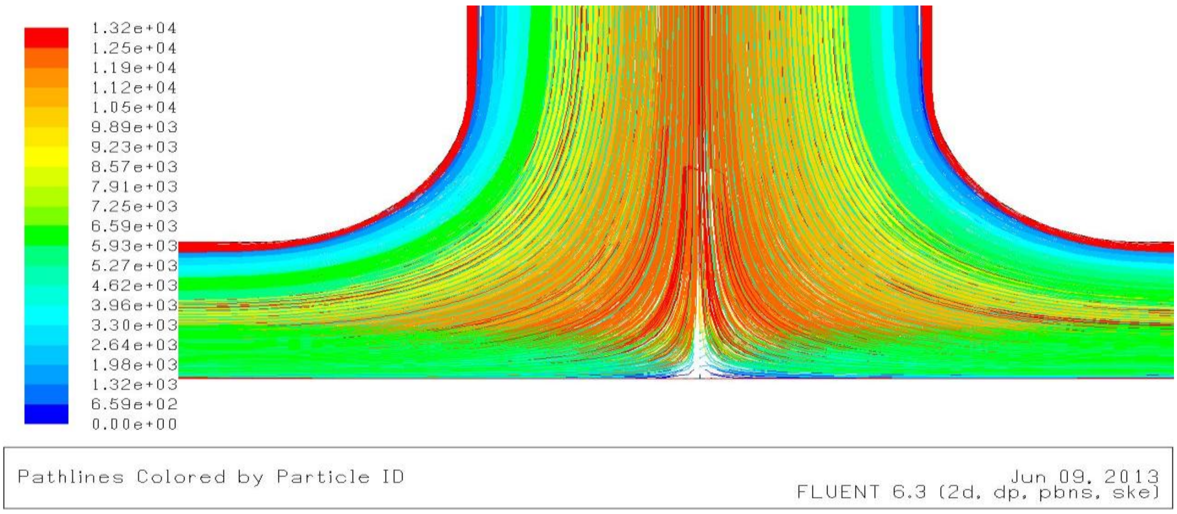

Figure 5.15: path lines for electrolyte flow path with corner radius of 0.9mm at inlet velocity, V=5m/s [$k-\varepsilon$ model with standard wall functions]

LIST OF TABLES

Table 5.1: showing possibility of vortex formation and negative pressure for sharp corners flow path

S.N.	Inlet velocity (m/s)	Model and wall function used in FLUENT	Reynolds Number (R_N)	Negative pressure inside flow path	Vortex formation
1.	5	$k-\varepsilon$ model with standard wall function	10500	YES	YES
2.	5	$k-\varepsilon$ model with Enhanced wall treatment	10500	YES	YES
3.	15	$k-\varepsilon$ model with standard wall function	31500	YES	YES
4.	15	$k-\varepsilon$ model with Enhanced wall treatment	31500	YES	YES
5.	30	$k-\varepsilon$ model with standard wall function	63000	YES	YES
6.	30	$k-\varepsilon$ model with Enhanced wall treatment	63000	YES	YES
7.	50	$k-\varepsilon$ model with standard wall function	105000	YES	YES
8.	50	$k-\varepsilon$ model with Enhanced wall treatment	105000	YES	YES

Table 5.2: showing possibility of vortex formation and negative pressure for flow path corners having radius of 0.6mm

S.N.	Inlet velocity (m/s)	Model and wall function used in FLUENT	Reynolds Number (R_N)	Negative pressure inside flow path	Vortex formation
1.	5	$k-\varepsilon$ model with standard wall function	10500	NIL	NIL
2.	5	$k-\varepsilon$ model with Enhanced wall treatment	10500	NIL	NIL
3.	15	$k-\varepsilon$ model with standard wall function	31500	NEGLIGIBLE	NEGLIGIBLE

4.	15	$k-\varepsilon$ model with Enhanced wall treatment	31500	NEGLIGIBLE	NEGLIGIBLE
5.	30	$k-\varepsilon$ model with standard wall function	63000	YES	NEGLIGIBLE
6.	30	$k-\varepsilon$ model with Enhanced wall treatment	63000	YES	NEGLIGIBLE
7.	50	$k-\varepsilon$ model with standard wall function	105000	YES	NEGLIGIBLE
8.	50	$k-\varepsilon$ model with Enhanced wall treatment	105000	YES	NEGLIGIBLE

Table 5.3: showing possibility of vortex formation and negative pressure for flow path corners having radius of 0.7mm

S.N.	Inlet velocity (m/s)	Model and wall function used in FLUENT	Reynolds Number (R_N)	Negative pressure inside flow path	Vortex formation
1.	5	$k-\varepsilon$ model with standard wall function	10500	NIL	NIL
2.	5	$k-\varepsilon$ model with Enhanced wall treatment	10500	NIL	NIL
3.	15	$k-\varepsilon$ model with standard wall function	31500	YES	NEGLIGIBLE
4.	15	$k-\varepsilon$ model with Enhanced wall treatment	31500	YES	NEGLIGIBLE
5.	30	$k-\varepsilon$ model with standard wall function	63000	YES	NEGLIGIBLE
6.	30	$k-\varepsilon$ model with Enhanced wall treatment	63000	YES	NEGLIGIBLE
7.	50	$k-\varepsilon$ model with standard wall function	105000	YES	NEGLIGIBLE
8.	50	$k-\varepsilon$ model with Enhanced wall treatment	105000	YES	NEGLIGIBLE

Table 5.4: showing possibility of vortex formation and negative pressure for flow path corners having radius of 0.8mm

S.N.	Inlet velocity (m/s)	Model and wall function used in FLUENT	Reynolds Number (R_N)	Negative pressure inside flow path	Vortex formation
1.	5	$k-\varepsilon$ model with standard wall function	10500	NIL	NIL
2.	5	$k-\varepsilon$ model with Enhanced wall treatment	10500	NIL	NIL
3.	15	$k-\varepsilon$ model with standard wall function	31500	NIL	NIL
4.	15	$k-\varepsilon$ model with Enhanced wall treatment	31500	NIL	NIL
5.	30	$k-\varepsilon$ model with standard wall function	63000	YES	NEGLIGIBLE
6.	30	$k-\varepsilon$ model with Enhanced wall treatment	63000	YES	NEGLIGIBLE
7.	50	$k-\varepsilon$ model with standard wall function	105000	YES	NEGLIGIBLE
8.	50	$k-\varepsilon$ model with Enhanced wall treatment	105000	YES	NEGLIGIBLE

Table 5.5: showing possibility of vortex formation and negative pressure for flow path corners having radius of 0.9mm

S.N.	Inlet velocity (m/s)	Model and wall function used in FLUENT	Reynolds Number (R_N)	Negative pressure inside flow path	Vortex formation
1.	5	$k-\varepsilon$ model with standard wall function	10500	NIL	NIL
2.	5	$k-\varepsilon$ model with Enhanced wall treatment	10500	NIL	NIL
3.	15	$k-\varepsilon$ model with standard wall function	31500	YES	NEGLIGIBLE

4.	15	$k-\varepsilon$ model with Enhanced wall treatment	31500	NIL	NIL
5.	30	$k-\varepsilon$ model with standard wall function	63000	YES	NEGLIGIBLE
6.	30	$k-\varepsilon$ model with Enhanced wall treatment	63000	YES	NEGLIGIBLE
7.	50	$k-\varepsilon$ model with standard wall function	105000	YES	NEGLIGIBLE
8.	50	$k-\varepsilon$ model with Enhanced wall treatment	105000	YES	NEGLIGIBLE

REFERENCES

[1] Ghosh and Mallik, Manufacturing Science, 2nd edition, EWP press, 2010

[2] Dr. D. S. Bilgi1, Mr. P. V. Jadhav2, Enhancement of surface finish of Pulse Electrochemically Machined (PECM) surface using rotating electrode. *International Journal of Computer Communication and Information System (IJCCIS)– Vol2. No1. ISSN: 0976–1349 July – Dec 2010*

[3] J. Kozak, mathematical model for computer simulation of electrochemical machining processes. Journal of Material Processing Technology 76(1998) 170-175.

[4] Jerzy kozak, Antoni F. Budzynski, PiotrDomanowski, Computer simulation electrochemical shaping (ECM-CNC) using a universal tool electrode. Journal of Material Technology 76(1998) 162-164.

BIBLIOGRAPHY

1. www.sciencedirect.com

2. www.nitrkl.ac.in

3. Computational fluid dynamics by H.Choi, H.G.Choi and J.Y.YOO (EDS)

4. Text book of Production technology HMT.